

Influences of Space Irradiations on the Structure and Properties of MoS₂/DLC Lubricant Film

Yanxia Wu¹ · Ying Liu¹ · Shengwang Yu¹ · Bing Zhou¹ · Bin Tang¹ · Hongxuan Li² · Jianmin Chen²

Received: 28 March 2016 / Accepted: 12 September 2016 / Published online: 30 September 2016
© Springer Science+Business Media New York 2016

Abstract This work aims at revealing the influences of space irradiations [including the atomic oxygen (AO) and ultraviolet (UV) irradiations] on the MoS₂/DLC solid lubricating film. The changes on microstructure, mechanical and vacuum tribological properties of nanocomposite films after irradiations have been systematically investigated. It is found that the AO irradiation mainly induces the surface oxidation of the film, whereas some oxygen atoms can erode the bulk film along the defects highway; thus, the connectivity of carbon atoms is improved. In contrast, the UV irradiation may break the carbon bonds and functional groups, as well as induce a secondary radical formation, which accelerates the broken and recombination of the carbon chain scission. Specially, the films after irradiations exhibit much higher hardness (>19 GPa), lower friction coefficient (<0.02) and wear rate compared with the original one. The excellent tribological properties of the films after irradiations can be attributed to the synergistic effect of the high *sp*³ C content and good crystallization of MoS₂ in the film, which cause the lower carbon and higher MoS₂ content in the wear debris at the contact interface.

Keywords MoS₂/DLC composite film · Atomic oxygen irradiation · Ultraviolet irradiation · Microstructure · Vacuum tribological properties

1 Introduction

The human exploration of the space environment is critically dependent on the correct and reliable operation of many moving mechanical assemblies and tribological components [1, 2]. However, most of these devices require low and stable friction and low wear rate, taking into account the need of low consumption, good reliability in some extreme operation conditions, such as ultra-high vacuum, the absence of gravity, AO irradiation and UV irradiation [3, 4]. It is essential, therefore, to select the right lubrication technique and lubricant for each device operated in space. Unfortunately, since the friction coefficient and wear life of the traditional solid lubricant vary with the environments [5, 6], no single solid lubricant exists or has been validated that meets these requirements so far. The development of new lubricant for these applications is still an urgent need.

Recently, diamond-like carbon (DLC) film is referred as a kind of potential space lubricant material due to its high hardness, low friction and wear rate [7, 8]. But the applications of pure DLC film in space environment are limited because of the adhesion, and cold-welding often occurs between the film and the counterpart under high vacuum, which can result in a high friction coefficient and short sliding lifetime [9]. Alternatively, recent studies on the doped DLC film and DLC-based solid–liquid synergistic lubricating coatings can improve the tribological properties of DLC film in vacuum [10–13]. Nevertheless, these works are mainly focused on the tribological

✉ Yanxia Wu
wuyanxia01@tyut.edu.cn

✉ Ying Liu
Liuying01@tyut.edu.cn

¹ College of Materials Science and Engineering, Taiyuan University of Technology, Taiyuan 030024, People's Republic of China

² State Key Laboratory of Solid Lubrication, Lanzhou Institute of Chemical Physics, Chinese Academy of Sciences, Lanzhou 730000, People's Republic of China

properties of the films in vacuum, and the influences of the space irradiations, such as AO and UV irradiations, are merely reported.

As is known, the space irradiations can alter the chemical structure of materials through decomposition and cross-links of chemical bonds, as well as exert significant influence on the tribological behaviors of lubricating materials. Herein, as a potential space lubricant, it is significant to study the influences of the space irradiations on the DLC-based films. In recent years, several literatures reported that the DLC-based films could exhibit excellent degradation resistant behaviors and good tribological properties after space irradiations. Ji et al. [14, 15] studied the effect of AO irradiation on the structure and properties of the Mo doped DLC film and found that Mo doped DLC film exhibited good tribological properties in dry Ar environment. Liu et al. [9] investigated the effects of AO and UV proton and electron irradiations on the structure and tribological properties of the DLC-based solid–liquid lubricating coating and found that the friction coefficient of the solid–liquid lubricating coatings decreased (except for AO irradiation) in high vacuum. However, the sliding lifetimes of these lubricating coating after irradiations in vacuum are not given longer than 1800 s, namely a further improvement on the tribological properties of the DLC-based lubricating films.

On the one hand, our previous studies have shown that the MoS₂ nanocrystalline doped DLC composite film could exhibit excellent tribological behaviors with a sliding lifetime longer than 3600 s in high vacuum [10]. On the other hand, Mo oxide nanostructures, which are formed by the oxidation of MoS₂ nanocrystalline under AO irradiation, not only can play as a protective layer against further atomic oxygen attack, but also offer a unique opportunity to produce adaptive or smart tribological coatings for the doped films [16, 17]. Thus, the nanostructured MoS₂/DLC film is considered to be a better space lubricant compared with the previously reported DLC-based lubricating coatings. However, to the best of our knowledge, there are few reports on the vacuum tribological behaviors of the MoS₂/DLC composite film after space irradiations.

Herein, this work is aimed at investigating the influences of AO and UV irradiations on the vacuum tribological performances of MoS₂/DLC lubricating film. The nanocomposite films are fabricated by unbalanced magnetron sputtering. The composition, microstructure, surface morphology, mechanical and tribological performances of the films before and after AO and UV irradiations have been systematically investigated. Furthermore, the internal mechanisms related to the enhanced tribological properties of the MoS₂/DLC film after space irradiations are also discussed.

2 Experimental

2.1 Deposition of the MoS₂/DLC Composite Film

The MoS₂/DLC composite films were prepared by unbalanced magnetron sputtering, and the details of the deposition system were described elsewhere [18]. The composite films were deposited on the stainless steel (for frictional tests) and Si substrates (for characterization), respectively. The deposition details of MoS₂/DLC film were as follows: (1) The sputtering current of C and MoS₂ was 14 and 0.8 A, respectively; (2) the applied pulsed negative voltage was 150 V with a duty cycle of 10 %; and (3) the deposition pressure was 0.3 Pa with Ar flow rate of 55 sccm. The as-deposited films were 1.5 μm with a deposition time of 2 h. Furthermore, special samples for TEM analysis were grown directly on the freshly cleaved single-crystal NaCl wafers.

2.2 Irradiation Procedure

The space irradiations were performed in vacuum; the equipment and principle schematic illustration of AO irradiation were referred before [14]. The impingement kinetic energy of neutral AO beam was 5 eV, which was the same as the direct impact energy of AO to material surfaces in actual low Earth orbit (LEO) orbit. A typical atomic oxygen flux at the sample position was determined to be 6×10^{15} atoms/cm² s, and the exposure period was controlled at 120 min. The UV irradiation test chamber was maintained at 10^{-5} Pa, and the wavelength range was 115–400 nm. A typical UV energy flux at the sample position was determined to be about sextuple of the solar constant, and the exposure period was controlled as 120 min, being equivalent to 12 sun hours.

2.3 Characterizations of the Films

The transmission electron microscopy (TEM) images of the nanocomposite film before irradiation were obtained by a JEM 2010 TEM operated at 300 kV. The surface chemical composition of the films was determined by a multifunctional X-ray photoelectron spectroscope (XPS, operating with Al-K α radiation and detecting chamber pressure below 10^{-8} torr). The oxygen adsorption contaminants on the film surface had not been removed in order to compare the AO-induced varieties of the surface chemical composition. A Jobin-Yvon HR-800 Raman spectrometer (excitation wavelength: 532 nm; power density on samples: 0.3 mW/m²) was used to analyze the structure of the films and the transfer film. The surface morphologies of the films were observed by atomic force

microscope (AFM, SEIKO SPA-300HV). The cross-sectional morphologies of the film were imaged with field emission scanning electron microscopy (FESEM, Hitachi S4800).

The hardness values of the films were determined by a NanoTest 600 nanomechanical system (MicroMaterials Ltd, UK), on which the maximum indentation depth was about 150 nm to minimize the effect of the substrate. The internal stress of the composite films had been calculated based on the Stoney equation [13], while the curvature radii were measured by a MicroXAM surface mapping microscope (ADE shift, America).

2.4 Friction Testing

The tribological properties of the composite films were evaluated with a ball-on-disk tribometer in a vacuum chamber. The sliding tests of the films against steel ball counterpart (GCr15, \varnothing 6 mm) were run at a normal load of 5 N (theoretical initial Hertzian contact pressure of 1.0 GPa), a sliding speed of 5 rev/s, a room temperature of about 20 °C and a maximum sliding duration of 3600 s, while the wear track radius was fixed at 6 mm. As the friction and wear tests in vacuum environment, a pressure of about 5.0×10^{-3} Pa was attained in the chamber with a turbomolecular pumping system. Each test was repeated three times. The morphology of the wear scar and wear track was characterized by a S. VEGA 3SBH scanning electron microscope (SEM), and the wear volume was observed using a JSM5910 3D non-contact surface profilometer.

3 Results and Discussion

3.1 Chemical Composition and Structure of the MoS₂/DLC Film

Figure 1 exhibits the TEM bright-field images of the as-deposited MoS₂/DLC film. It is shown that the composite film has a typical nanocomposite structure, in which the MoS₂ nanoparticles (about 5 nm) are embedded in the cross-linked amorphous carbon matrix.

The XPS spectra of the composite film before and after the AO and UV irradiations are shown in Fig. 2. It can be seen from Fig. 2a that the C1s spectrum of the original film is fitted into three components at 284.4, 285.3 and 286.3 eV, respectively. The main peak at 284.4 eV is corresponded to the sp^2 C=C bond, whereas the other two peaks with smaller intensities at 285.3 and 286.3 eV are ascribed to sp^3 C–C and C–O bonds, respectively. The formation of sp^3 C–O bonding can be attributed to the contaminants formed on the surface of the film due to the

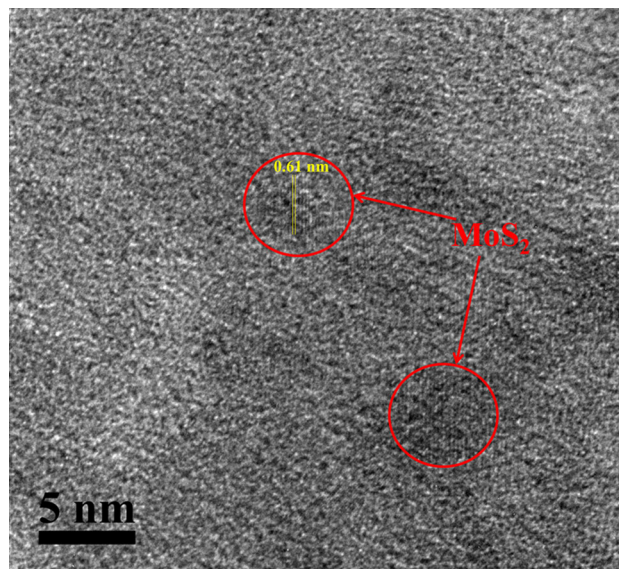
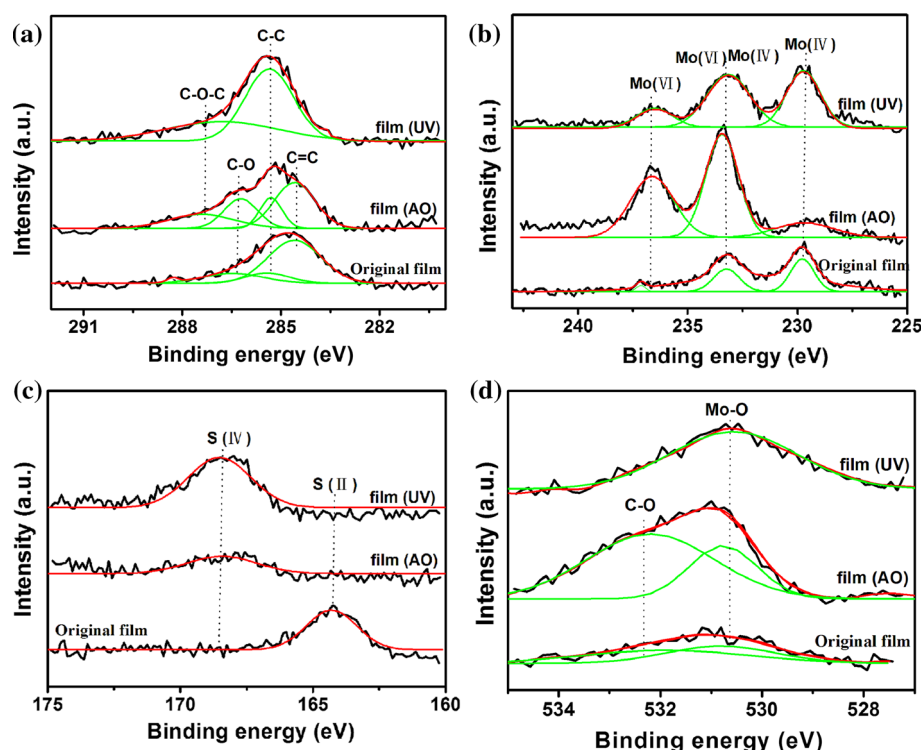


Fig. 1 TEM image of the as-deposited MoS₂/DLC composite film

air exposure. However, the bond structure of the film changes greatly after irradiations. For the AO-irradiated film, the intensities of the peaks identified as sp^3 C–C and C–O bonds increase significantly as the sp^2 C=C bond decreases. Furthermore, the fourth peak located at 287.3 eV is corresponded to the C–O–C bond. These peaks are mainly resulted from the reaction between the carbon and oxygen atoms on the surface of the film [9, 16]. In the chemically active atomic oxygen environment, sp^3 C sites with free σ -bonds on the surface preferentially react with the O atoms and form volatile CO and CO₂, while some of the sp^2 C sites may combine with O atoms and form C–O–C bonds. Because of the destroyed carbon rings in DLC matrix, the sp^3 C content increases when the sp^2 C content decreases. As concerning the UV-irradiated film, there exist two components assigned to the sp^3 C–C and C–O–C bonds, respectively. The UV irradiation is energetic enough to break the carbon bonds and functional groups, such as C=C and C=O bonds [19]. Simultaneously, it may induce a secondary radical formation, which accelerates the broken and recombination of the carbon chain scission [15, 20]. As a result, some of the destroyed sp^2 C bonds recombine and form the sp^3 hybridized carbon bonds, inducing the increased sp^3 C–C bonds in turn.

Figure 2b shows the Mo3d spectra of the composite film before and after irradiations. Generally, the peak located at 229.3 eV is related to the Mo–S bond in MoS₂, whereas the Mo3d doublet at 232.5 and 236.4 eV is corresponded to Mo(VI) in MoO₃ [16, 21]. The spectrum of the original film shows that the Mo atoms in the composite film are mainly combined with S. But some of the Mo atoms are oxidized to Mo(VI) state after AO irradiation, and the Mo(VI) state increases a little after UV irradiation.

Fig. 2 XPS spectra of the MoS₂/DLC composite film before and after the AO and UV irradiations: **a** the C1s, **b** Mo3d, **c** O1s and **d** S2p



Compared with the S2p spectra in Fig. 2c, it can be seen that the S atoms are oxidized after the irradiations with the peak located at 164.1 shifting to 168.5 eV, and there are much more S atoms in S(IV) state after UV irradiation than that after AO irradiation. This is originated from the oxidation and bonding of S atoms with atomic oxygen in AO irradiation, and the formed SO and SO₂ gasify to the surrounding circumstances. Consequently, the oxidized S atoms decrease when the Mo(VI) state increases greatly in the AO irradiation environment. In contrast, the oxidation of Mo and S atoms in the UV irradiation process is slight. Some SO₂ can be formed and aggregated on the surface of film, which lead to a little increase in Mo(VI) state and a great increase in S(IV) state. Combining the Mo3d, S2p spectra with O1s spectra in Fig. 2d, it can be concluded that the film surface is oxidized seriously after AO irradiation, on which a large number of C–O and Mo–O bonds are formed. While after UV irradiation, the oxidation is slight and there are Mo–O bonds formed on the film surface. This indicates that the uniformly dispersed MoS₂ nanoparticles can react preferentially with the atomic oxygen owing to their high affinity with oxygen atoms and finally form some MoO₃ produces on the film's surface.

Raman spectroscopy is a popular and effective way to distinguish the microstructural characteristics of DLC-based films [22]. Figure 3a shows the Raman spectra of the MoS₂/DLC films before and after the AO and UV irradiations. The peaks at 178, 350, 400 and 721 cm⁻¹ can be characterized as MoS₂ nanoparticles, and those around 200

and 928 cm⁻¹ are assigned to MoO₃. Furthermore, the broad peak in the region between 1300 and 1500 cm⁻¹, which can be fitted into two peaks by Gaussian function, is the characteristic of DLC film. The G peak around 1550 cm⁻¹ is ascribed to the bond stretching of all pairs of sp² carbon atoms in both rings and chains, while the D peak around 1350 cm⁻¹ is attributed to the breathing modes of sp² carbon atoms in rings. Previous studies have shown that the G peak shift and the intensity ratio for the D and G peaks (I_D/I_G ratios) can provide effective information on the structure of carbon-based film [18]. Gaussian fit of the spectra exhibiting the G and D peak within 1050–2000 cm⁻¹ region is given in Fig. 3b. The corresponding wave number of the G peak position as well as the I_D/I_G ratio for the films before and after irradiations is given in Table 1. The G peak position shifts to a lower wave number when the I_D/I_G ratio decreases after irradiations. It indicates a decreased sp² cluster size and increased sp³ fraction after irradiations. Meanwhile, the peaks corresponded to MoS₂ become sharper, implying the MoS₂ is well crystallized in the film after irradiations. Yet the changes of peaks identified as MoO₃ are not obvious, especially for the film after AO irradiation; the oxidation of MoS₂ mainly occurs on the surface of the film. Previous studies have demonstrated that proper laser irradiation can improve the crystallinity of composite film [23, 24], and our work further proves that proper AO or UV irradiations will enhance the crystallinity of MoS₂ nanoparticles in the composite film.

Fig. 3 Raman spectra of the MoS₂/DLC composite film before and after the AO and UV irradiations: **a** the full spectra; **b** spectra exhibiting the G and D fittings in the region of 1050–2000 cm⁻¹

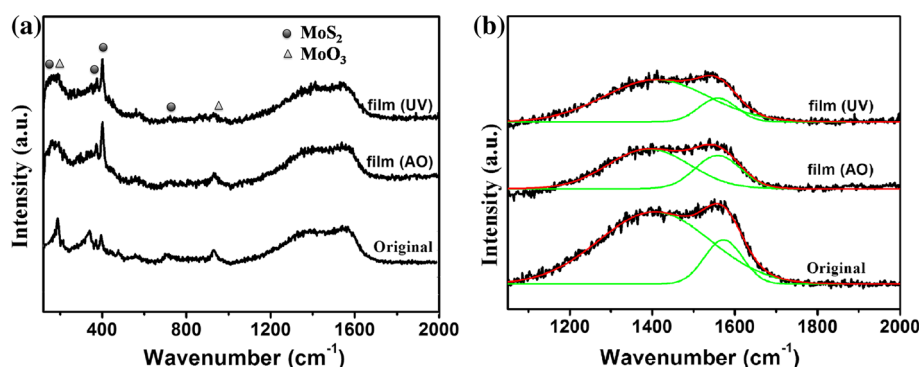


Table 1 The G peak positions and the corresponding I_D/I_G ratios of the MoS₂/DLC films before and after the AO and UV irradiations

	Original	Film (AO)	Film (UV)
G peak position (cm ⁻¹)	1565	1558	1557
I_D/I_G ratio	3.57	2.13	3.09

Based on the Raman and XPS spectra of the MoS₂/DLC films before and after the AO and UV irradiations, it is identified that the AO irradiation can induce an increasing sp^3 C fraction in the film. The active oxygen atoms and ions in the AO environments not only can attack the surface of the film, but also erode the bulk film. Previous research has reported that the defects in the MoS₂ composite film can provide a reaction highway, which allows the incident atomic oxygen to enter into the bulk film and react with the sulfur atoms distributed within irregular cavities [25]. Thus, it is speculated that the oxygen may attack the bulk film along with the defects highway and combine with C atoms in an AO-irradiated environment with high oxygen fluence. Meanwhile, the irradiation can give rise to extreme pressure inside carbon-based nanoparticle or carbon rings in the film, so that these systems can be used as compression cells to induce high-pressure transformations of materials. Diamond crystals can be nucleated and grown in these systems, which can cause high sp^3 C content in turn [26]. As a result, the coordination number of carbon atom increased, and the connection of carbon network was improved further. On the other hand, the increased sp^3 C fraction in the film after UV irradiation is caused by the recombination of sp^2 C rings, which can be easily broken, but difficult to recover under the UV irradiation environment. Furthermore, the formed radicals by broken carbon bonds, such as C–C, C=C and C=O, are inclined to migrate and recombine with other components, thus increasing the cross-linking of DLC matrix.

Figure 4 presents the AFM images of MoS₂/DLC films before and after the AO and UV irradiations over an area of

8.0 $\mu\text{m} \times 8.0 \mu\text{m}$. It is seen that all the films have relatively compact and rough surfaces. The original and UV-irradiated films exhibit granular structure with small particle size, whereas the film after AO irradiation obtains a larger grain structure due to the increased content of MoO₃ [27]. Additionally, the emission of some degradation products caused by the bombardment during irradiations may also raise a rougher surface [14].

Figure 5 shows the corresponding cross-sectional FESEM micrographs of the MoS₂/DLC composite films before and after the AO and UV irradiations. The composite film mainly exhibits a compact structure. There are pores and destroyed block distributed in the film after AO irradiation, which means that the oxygen erosion process can easily diffuse along these defects pathway and erode the carbon matrix. Meanwhile, due to the recombination within the film structure, the film after UV irradiation shows much more dense and regular structure than that of the original one, namely an enhanced cross-linked of the carbon matrix.

The schematic structure of the MoS₂/DLC films before and after the AO and UV irradiations is given in Fig. 6. The main structure of the original composite film is consisted of MoS₂ nanocrystals and carbon matrix, which is composed of the sp^3 C and sp^2 C. Additionally, there is some oxygen absorbed and reacted with the elements on the surface. Considering the film after AO irradiation, the oxygen not only reacts with the elements on the surface, but also erodes the DLC matrix along with the defects, thus inducing the changes in microstructure of the film. However, for the UV-irradiated film, the UV irradiation mainly causes the conversion of carbon bonds, and an increasing sp^3 C content is obtained.

3.2 Mechanical Properties of the MoS₂/DLC Film

Table 2 shows the hardness and internal stress of the MoS₂/DLC films before and after the AO and UV irradiations. Compared with the original film (about 3.55 GPa), the hardness of the composite films after irradiations reaches

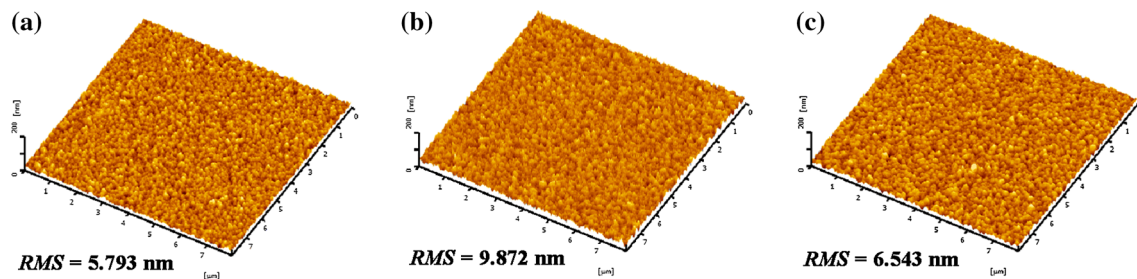


Fig. 4 AFM images of the MoS₂/DLC composite film before and after the AO and UV irradiations

Fig. 5 Cross-sectional FESEM micrographs of the film before and after the AO and UV irradiations

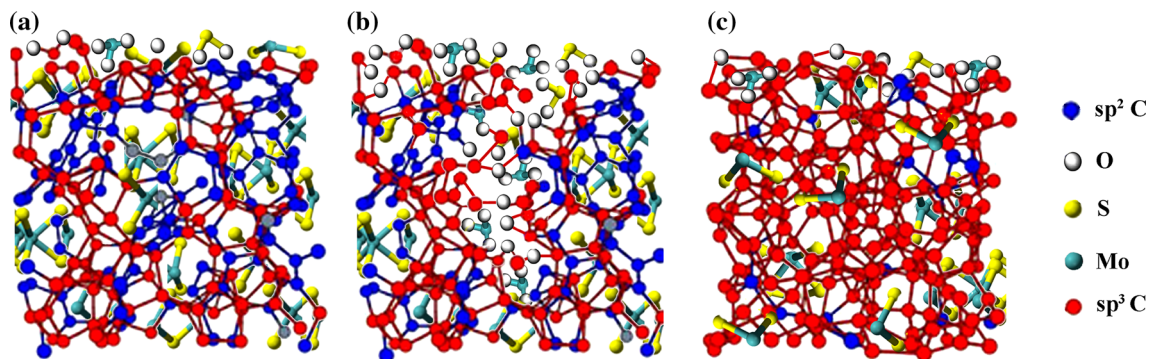
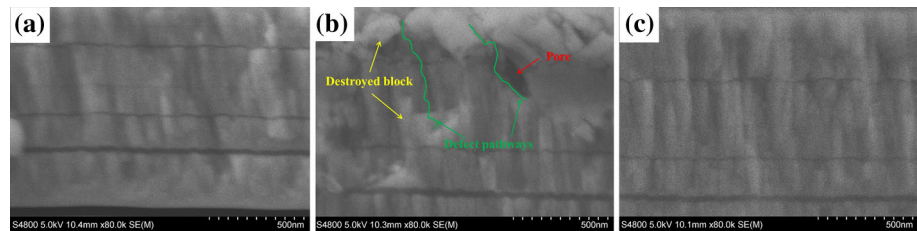


Fig. 6 The schematic structure of the films before and after the AO and UV irradiations

Table 2 Hardness and internal stress of the MoS₂/DLC films before and after the AO and UV irradiations

	Original	Film (AO)	Film (UV)
Hardness (GPa)	3.55	19.1	20.4
Internal stress (GPa)	0.426	1.314	1.545

the highest value of 20.4 GPa. This significant improvement is mainly attributed to the presence of a higher fraction of sp^3 bonds, which is favorable for the connectivity of carbon atoms in various existing sites and enhances the rigid carbon network after irradiations.

On the other hand, the internal stress of the films after AO and UV irradiations is 1.314 and 1.545 GPa, respectively, whereas that of the original one is just about 0.426 GPa. The enhanced internal stress for the irradiated films can also be revealed by the increasing sp^3 C bonds since it can strain the sp^2 C clusters in DLC matrix. Under

the AO irradiation, the oxygen atoms diffuse along the defects and bond with carbon, thus causing the twist or distortion of carbon network. But for the UV-irradiated film, the broken carbon chains in the carbon network are increased, as well as the cross-linkage of DLC matrix. Ultimately, all of these factors result in a high internal stress for the MoS₂/DLC films after irradiations.

3.3 Vacuum Tribological Properties of the MoS₂/DLC Film

The frictional curves of the composite films before and after the AO and UV irradiations in high vacuum are shown in Fig. 7. It can be seen that the films after irradiations maintain much steadier and lower friction coefficient in the steady-state period, as well as the sliding lifetime exceeds 3600 s, even though they exhibit higher friction coefficients in the run-in period. Specifically, because of the serious surface oxidation, the film after AO irradiation

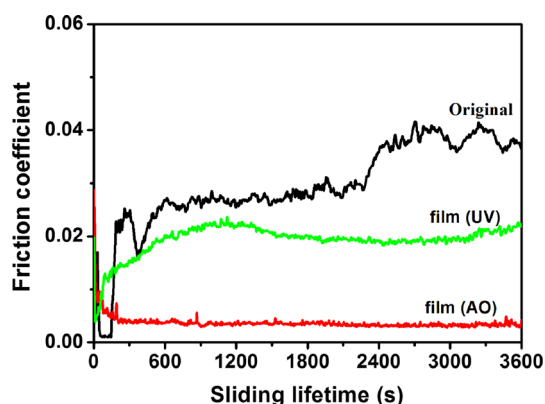


Fig. 7 Frictional curves of the MoS₂/DLC composite film before and after AO and UV irradiations in high vacuum

shows the highest friction coefficient during the first tens of seconds. But it obtains the lowest friction coefficient of 0.003 in vacuum. In contrast, the friction coefficient of the film after UV irradiation is in medium with a value of about 0.02, whereas the original film owns the highest one (about 0.03). Figure 8 shows the wear rate of the films before and after the AO and UV irradiations. It can be seen that the films after irradiations show much lower wear rate compared with the original one, indicating better wear resistance. Among them, the film after UV irradiation exhibits the best wear resistance.

To understand the wear mechanisms, the worn surface of the composite films as well as the counterpart ball is shown in Fig. 9. For the original MoS₂/DLC film (Fig. 9a, b), it can be seen clearly that the counterpart ball is covered by a thick and compact transfer film, where some debris are scattered in the wear track or around it. For the film after AO irradiation (Fig. 9c, d), no transfer film is formed on the counterpart ball, and few wear debris existed in the wear scar. However, after the UV irradiation (Fig. 9e, f), there is a torn transfer film on the counterpart ball, and the

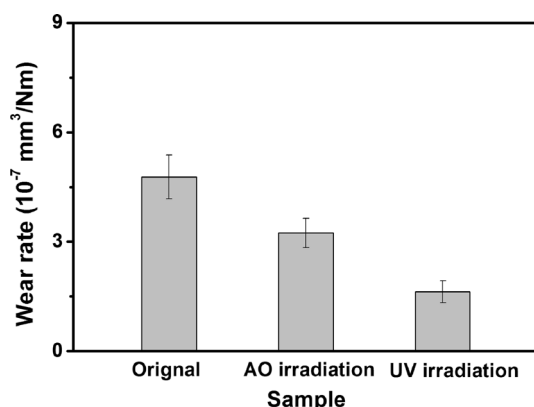


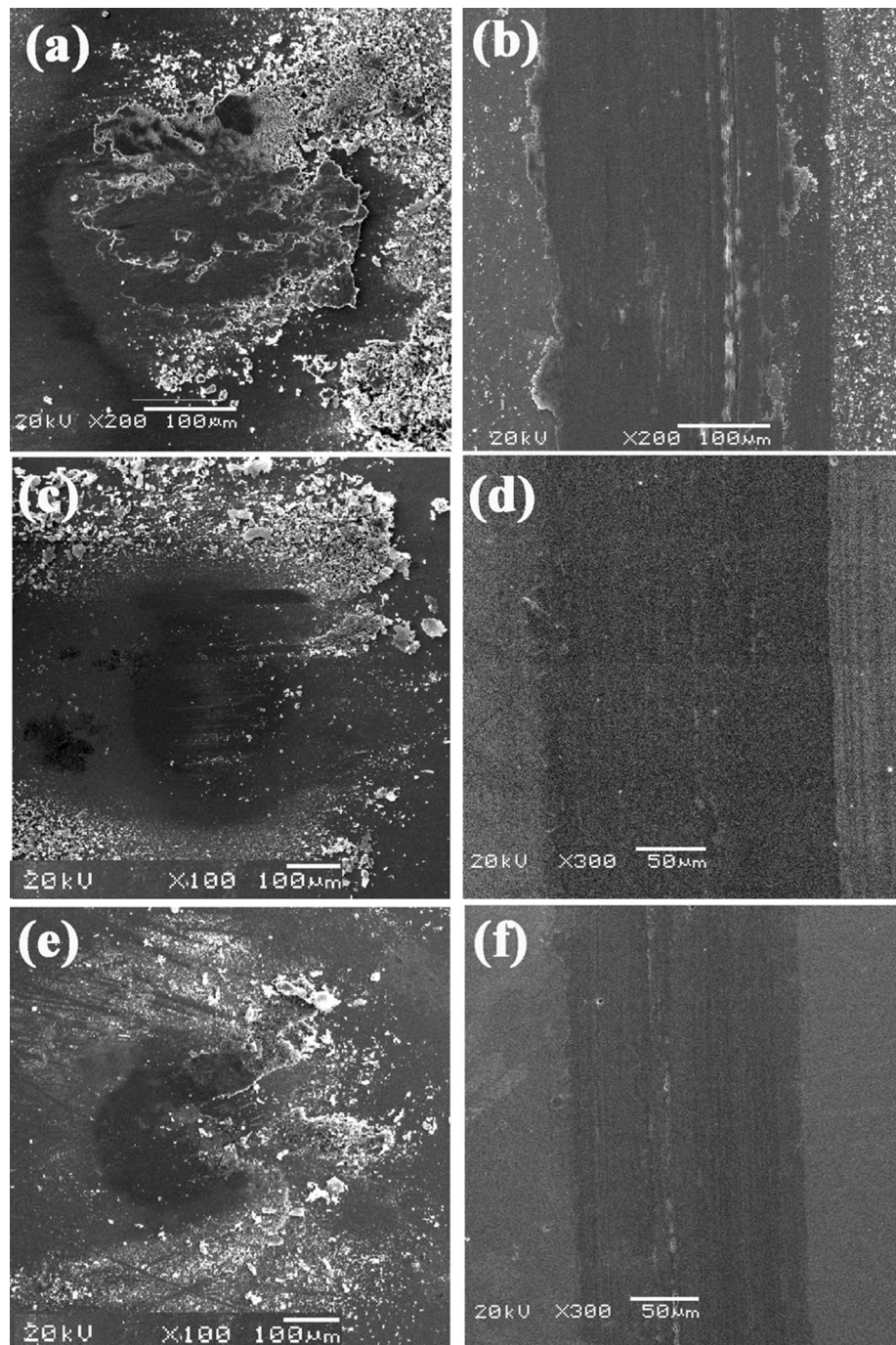
Fig. 8 Wear rates of the MoS₂/DLC composite film before and after AO and UV irradiations

wear track is the narrowest with few wear debris on it. The tribological properties of the original film can be interrupted as follows: The wear debris are trapped at the sliding contact interface and undergoes severe physical grinding action during friction, thus increasing the thickness of transfer film on the counterpart ball. The poor adhesion between the transfer film and the counterpart ball can result in a higher and fluctuated friction coefficient [8]. But for the films after irradiations, the narrower wear track with little wear debris indicates a lower wear rate. The lower friction coefficient can be related to the little grind wear debris on the counterpart ball.

In order to gain more insight into the friction and wear mechanisms of the MoS₂/DLC composite films, Raman spectra of the weak debris on the counterpart balls are shown in Fig. 10, respectively. Compared with Raman spectra of the bulk film (as shown in Fig. 2), there are no changes in the MoS₂ peaks and the relative peak intensity, which are identified as carbon for the original film. However, after irradiations, the relative intensities of the peaks assigned to carbon are decreased, indicating low carbon content on the counterpart ball. Furthermore, the intensities of peaks corresponded to MoS₂ at 179, 335, 401, 715 and 820 cm⁻¹ increase obviously, which indicates a higher MoS₂ content on the counterpart ball. Herein, it can be speculated that the excellent tribological properties for the films after irradiations are closely related to the high MoS₂ and low carbon contents at the contact interface. The carbon state in the wear debris is investigated further, and Table 3 shows the Gaussian fitting results of the carbon peaks. The G peak position shifts to a higher wave number when the I_D/I_G ratio increases (compared with Table 1). It illustrates the increasing graphitization of DLC matrix during the frictional tests. Simultaneously, the AO-irradiated film with the highest *sp*³ C content experiences the least graphitization during the test.

Combining the XPS spectra with Raman spectra (as shown in Figs. 2, 3, 10), it can be found that the irradiations initiate raise in both the crystallization of MoS₂ and content of *sp*³ C. With increasing *sp*³ C in the film, the rigidity and strength of the carbon network increased, which provides a high load-bearing capacity and good wear resistance. On the other hand, the MoS₂ with better crystallization is inclined to maintain low shear strength during the frictional test in vacuum. As a result, the film after irradiations exhibits better tribological properties. Additionally, there are three main reasons for the different wear rates of the films after AO and UV irradiations. Firstly, the wear rate of a given film is closely related to its hardness. A harder film can provide higher bearing capacity and thus reduce the wear rate. Secondly, the wear rate of a lubricating film is closely related to its surface roughness. The

Fig. 9 SEM images of worn surface for the MoS₂/DLC composite film and the corresponding counterpart ball before and after irradiations: **a**, **b** the as-deposited film, **c**, **d** after the AO irradiation and **e**, **f** after the UV irradiation



higher roughness the DLC film shows the greater wear the film maintains. Thirdly, the graphitization of DLC matrix during friction can also aggravate the wear of the films. The overall wear rate is a balance of these factors. The

highest wear rate of the original film is closely related to its lowest hardness, while the lowest wear rate for the film after UV irradiation can be attributed to its highest hardness and relatively lower roughness.

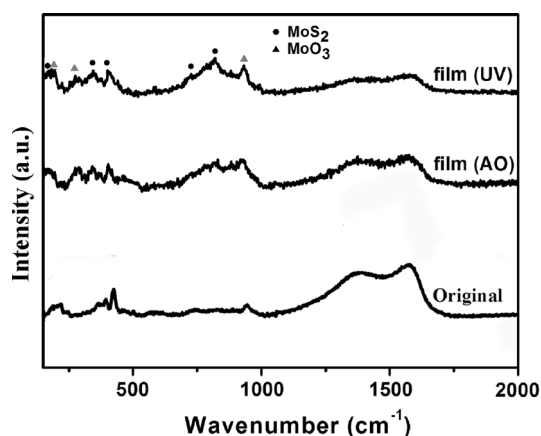


Fig. 10 Raman spectra of the wear debris on counterpart ball for the MoS₂/DLC film before and after AO and UV irradiations

Table 3 The G peak position and the corresponding I_D/I_G ratio of the wear debris on the counterpart ball

	Original	Film (AO)	Film (UV)
G peak position (cm ⁻¹)	1578	1580	1578
I _D /I _G ratio	3.85	3.36	3.77

4 Conclusions

The effects of the AO and UV irradiations on the composition, microstructure, morphology, mechanical and vacuum tribological properties of the MoS₂/DLC composite film have been investigated. Results show that both the irradiations can increase the *sp*³ C content and MoS₂ crystalline of the film. The AO irradiation mainly induces the surface oxidation of the film. Specially, some oxygen may erode the bulk film along with the defect highway and connect the carbon atoms in the matrix. In contrast, the UV irradiation leads to the broken *sp*² carbon rings and recombination of free radicals, which improves the cross-linking of DLC matrix in turn. Compared with the original one, the films after irradiations exhibit much higher hardness (>19 GPa) and better vacuum tribological properties with a friction coefficient less than 0.02 and wear rate lower than 4×10^{-7} mm³/Nm. The enhanced tribological properties of the composite film can be attributed to the synergistic effect of high *sp*³ C content and good MoS₂ crystallization in the films after irradiations. Furthermore, the highest wear rate of the original film is closely related to its lowest hardness, while the lowest wear rate for the film after UV irradiation can be attributed to its highest hardness and relatively lower roughness.

Acknowledgments The authors thank the National Natural Science Foundation of China (Grant No. 51505318) and the Youth Foundation of Taiyuan University of Technology (No. 1205-04020102) for financial support.

References

1. Roberts, E.W.: Space tribology: its role in spacecraft mechanisms. *J. Phys. D Appl. Phys.* **45**, 503001 (2012)
2. Sathyan, K., Hsu, H.Y., Lee, S.H., Gopinath, K.: Long-term lubrication of momentum wheels used in spacecrafts—an overview. *Tribol. Int.* **43**, 259–267 (2010)
3. Fontaine, J., Donnet, C., Le Mogne, T., Belin, M., Berthier, Y., Heau, C., Terrat, J.P., Pont, G.: Towards the solid lubrication of space mechanisms by diamond-like carbon coatings. *ESA-SP* **438**, 297–302 (1999)
4. Krick, B.A., Sawyer, W.G.: Space tribometers: design for exposed experiments on orbit. *Tribol. Lett.* **41**, 303–311 (2011)
5. Scharf, T.W., Prasad, S.V.: Solid lubricants: a review. *J. Mater. Sci.* **48**, 511–531 (2013)
6. Wood, R.J.K.: Tribo-corrosion of coatings: a review. *J. Phys. D Appl. Phys.* **40**, 5502 (2007)
7. Paul, R., Das, S.N., Dalui, S., Gayen, R.N., Roy, R.K., Bhar, R., Pal, A.K.: Synthesis of DLC films with different *sp*²/*sp*³ ratios and their hydrophobic behaviour. *J. Phys. D Appl. Phys.* **41**, 055309 (2008)
8. Erdemir, A., Donnet, C.: Tribology of diamond-like carbon films: recent progress and future prospects. *J. Phys. D Appl. Phys.* **39**, R311 (2006)
9. Liu, X., Wang, L., Pu, J., Xue, Q.: Surface composition variation and high-vacuum performance of DLC/ILs solid-liquid lubricating. *Appl. Surf. Sci.* **258**, 8289–8297 (2012)
10. Wu, Y., Li, H., Ji, L., Ye, Y., Chen, J., Zhou, H.: A long-lifetime MoS₂/a-C:H nanoscale multilayer film with extremely low internal stress. *Surf. Coat. Technol.* **236**, 438–443 (2013)
11. Liu, X., Pu, J., Wang, L., Xue, Q.: Novel DLC/ionic liquid/graphene nanocomposite coatings towards high-vacuum related space applications. *J. Mater. Chem. A* **1**, 3797–3809 (2013)
12. Wu, Y., Li, H., Ji, L., Ye, Y., Chen, J., Zhou, H.: Preparation and properties of MoS₂/a-C films for space tribology. *J. Phys. D Appl. Phys.* **46**, 425301 (2013)
13. Wu, Y., Li, H., Ji, L., Liu, L., Ye, Y., Chen, J., Zhou, H.: Structure, mechanical, and tribological properties of MoS₂/a-C:H composite films. *Tribol. Lett.* **52**, 371–380 (2013)
14. Ji, L., Li, H., Zhao, F., Quan, W., Chen, J., Zhou, H.: Atomic oxygen resistant behaviors of Mo/diamond-like carbon nanocomposite lubricating films. *Appl. Surf. Sci.* **255**, 4180–4184 (2009)
15. Ji, L., Li, H., Zhao, F., Quan, W., Chen, J., Zhou, H.: Influences of ultraviolet irradiation on structure and tribological properties of diamond-like. *Appl. Surf. Sci.* **255**, 8409–8413 (2009)
16. Tagawa, M., Yokota, K., Matsumoto, K., Suzuki, M., Teraoka, Y., Kitamura, A., Belin, M., Fontaine, J., Martin, J.: Space environmental effects on MoS₂ and diamond-like carbon lubricating films: atomic oxygen. *Surf. Coat. Technol.* **202**, 1003–1010 (2007)
17. Voevodin, A.A., Zabinski, J.S.: Nanocomposite and nanostructured tribological materials for space applications. *Compos. Sci. Technol.* **65**, 741–748 (2005)
18. Wang, Y., Li, H., Ji, L., Liu, X., Wu, Y., Lv, Y., Fu, Y., Zhou, H., Chen, J.: Synthesis and characterization of titanium-containing graphite-like carbon films with low internal. *J. Phys. D Appl. Phys.* **45**, 295301 (2012)
19. Grossman, E., Gouzman, I.: Space environment effects on polymers in low earth orbit. *Nucl. Instrum. Methods Phys. Res. B* **208**, 48–57 (2003)
20. Skurat, V.: Vacuum ultraviolet photochemistry of polymers. *Nucl. Instrum. Methods Phys. Res. B* **208**, 27–34 (2003)

21. DiazDroguett, D.E., Fuenzalida, V.M.: Gas effects on the chemical and structural characteristics of porous MoO_3 and MoO_{3-x} grown by vapor condensation in helium and hydrogen. *Mater. Chem. Phys.* **126**, 82–90 (2011)
22. Zhao, F., Li, H.X., Ji, L., Mo, Y.F., Quan, W.L., Zhou, H.D., Chen, J.M.: Structural, mechanical and tribological characterizations of a-C:H:Si films prepared by a hybrid. *J. Phys. D Appl. Phys.* **42**, 165407 (2009)
23. Hirvonen, J.P., Koskinen, J., Jervis, J.R., Nastasi, M.: Present progress in the development of low friction coatings. *Surf. Coat. Technol.* **80**, 139–150 (1996)
24. Jervis, T.R., Nastasi, M., Bauer, R., Fleischauer, P.D.: Laser surface processing of molybdenum disulfide thin films. *Thin Solid Films* **181**, 475–483 (1989)
25. Wang, P., Qiao, L., Xu, J., Li, W., Liu, W.: Erosion mechanism of MoS_2 -based films exposed to atomic oxygen environments. *ACS Appl. Mater. Interfaces* **7**, 12943–12950 (2015)
26. Krasheninnikov, A.V., Banhart, F.: Engineering of nanostructured carbon materials with electron or ion beams. *Nat. Mater.* **6**(10), 723–733 (2007)
27. Hajakbari, F., Meibodi, A.E., Moghri Moazzen, M.A.: Influence of thermal oxidation temperatures on the structural and morphological properties of MoO_3 thin films. *Acta. Phys. Pol. A* **123**, 307–308 (2013)